OPEN ACCESS

Kashf Journal of Multidisciplinary Research
Vol: 02 - Issue 07 (2025)
P-ISSN: 3007-1992 E-ISSN: 3007-200X
https://kjmr.com.pk

NUMERICAL INVESTIGATION OF THE STATIC PHI-4 EQUATION USING A HYBRID CUBIC B-SPLINE TECHNIQUE

Ayesha Samra*
Faculty of Sciences, The Superior University, Lahore, Pakistan

Muhammad Amin
Faculty of Sciences, The Superior University, Lahore, Pakistan

Saima Mushtaq
Faculty of Sciences, The Superior University, Lahore, Pakistan

Nouman Iftikhar
Faculty of Sciences, The Superior University, Lahore, Pakistan

****Corresponding author:*** (ayesha.mnazakat@gmail.com)

Article Info

Abstract

The present work focuses on solving the one-dimensional static Phi-4 (ϕ^4) nonlinear differential equation using the Hybrid Cubic B-Spline (HCS) method. This nonlinear field equation arises in various physical contexts, including quantum field theory, phase transition models, and nonlinear optics. Traditional methods, such as finite difference or spectral techniques, face limitations in handling sharp transitions or ensuring smoothness across the domain. The HCS approach, a fusion of finite element and spline-based methods, offers high accuracy with smooth approximation. The mathematical derivation of the method, stiffness matrix construction, and implementation of boundary conditions are discussed in detail. Results are validated against the exact analytical kink solution, and the error analysis shows excellent agreement, confirming the efficacy of the method. This work emphasizes the stability, accuracy, and potential of HCS for solving nonlinear boundary value problems in mathematical physics.

Keywords:

Hybrid Cubic B-Spline Method, Static Phi-4 Equation. Nonlinear Differential Equation.

1. Introduction

The ϕ^4 model has long stood as a central topic in the study of nonlinear field equations due to its rich mathematical structure and broad applicability across disciplines such as quantum field theory, condensed matter physics, and statistical mechanics. Originally introduced as a simplified field-theoretic model to understand spontaneous symmetry breaking [1], the ϕ^4 equation exhibits a nonlinear interaction potential of the form

$$V(\phi) = \frac{\lambda}{4}\left(\phi^2 - \frac{m^2}{\lambda}\right)^2$$

giving rise to topologically stable solutions known as kinks [2, 3]. These kinks represent a transition between vacuum states and are essential in describing phenomena such as domain walls in ferromagnets, optical pulse propagation, and solitonic excitations in field theory [4].

In the one-dimensional static case, the ϕ^4 equation reduces to the second-order nonlinear boundary value problem:

$$\frac{d^2\phi}{dx^2} = \phi - \phi^3,$$

$$\phi(-L) = -1, \quad \phi(L) = 1.$$

This formulation admits an exact analytical solution:

$$\phi(x) = tanh\left(\frac{x}{\sqrt{2}}\right),$$

Which smoothly interpolates between the two vacuum states and , and is often used as a benchmark for validating numerical methods [5].

Traditional numerical approaches for solving such nonlinear differential equations include finite difference methods (FDM), spectral methods, and finite element methods (FEM) [6-8]. While FDM is easy to implement, it often lacks the accuracy needed to capture sharp transitions inherent in kink solutions. Spectral methods offer exponential convergence for smooth problems but can be sensitive to domain boundaries and require global basis functions, resulting in dense system matrices [9, 10]. FEM provides flexibility in handling complex domains but may still require mesh refinement to resolve steep gradients.

Cubic B-splines offer a compromise between local support, high-order smoothness, and ease of implementation [11, 12]. These functions are widely used in approximation theory, computer-aided design, and numerical PDEs. Their compact support leads to sparse system matrices, while their continuity ensures smooth representation of derivatives, a crucial property for solving second-order differential equations [13].

Recently, hybrid methods that integrate B-spline approximation within a Galerkin framework have gained attention due to their ability to handle nonlinearity with improved stability and accuracy [14-16]. The Hybrid Cubic B-Spline (HCS) method combines the strengths of B-spline interpolation and the variational principles underlying FEM to produce a method that is both accurate and efficient. Such methods have

been successfully applied to Bratu-type problems [17], reaction-diffusion systems [18], and Burgers' equation [19].

The motivation for using the HCS method in this study is driven by its ability to produce smooth, accurate approximations of nonlinear solutions while preserving computational efficiency. The local support of the B-spline basis also makes the method amenable to sparse matrix techniques, which reduce computational cost and storage requirements [20].

In this work, we develop a numerical scheme based on the HCS method to solve the static ϕ^4 equation. The main contributions are:

1. A complete derivation of the weak form of the ϕ^4 equation using Galerkin's method.
2. The incorporation of cubic B-spline basis functions to discretize the solution space.
3. Newton-Raphson iteration for solving the resulting nonlinear system.
4. Error analysis based and maximum norm comparisons with the exact solution.

Each component of this study is supported by existing literature on variational methods [21], spline theory [11], and nonlinear solvers [22, 23]. Through this approach, we aim to demonstrate that the HCS method provides a robust and accurate framework for solving nonlinear boundary value problems like the ϕ^4 equation.

Beyond the formulation and numerical strategy, particular attention must be paid to the robustness and convergence behaviour of the proposed method when applied to strongly nonlinear regimes. Since the ϕ^4 equation introduces significant nonlinearity through the cubic term in the potential, even minor numerical artifacts can lead to instability or loss of accuracy in conventional schemes. In contrast, the hybrid B-spline approach exhibits superior resilience against such difficulties due to its high smoothness and compact support, effectively mitigating oscillations and promoting stability without requiring excessively fine discretization [24, 25].

Moreover, the Newton-Raphson iterative solver employed in this work is particularly well-suited for the ϕ^4 model's nonlinear structure. By incorporating the exact Jacobian of the residual function within the iteration scheme, convergence is accelerated, and computational effort is reduced [26, 27]. Coupling this solver with the hybrid cubic B-spline representation ensures that both the spatial and nonlinear characteristics of the system are treated with a high degree of fidelity.

An integral part of this investigation also involves quantifying the deviation between numerical and analytical solutions. To this end, various error metrics, including maximum norm and L^2 -norm errors, are computed. These metrics not only provide a benchmark for performance but also highlight the practical efficacy of the HCS method across varying grid resolutions and boundary conditions [28, 29].

1.1 Fractional Derivative with Caputo-Fabrizio Kernel

In recent developments in fractional-order modeling, the Caputo-Fabrizio (CF) fractional derivative has become prominent due to its non-singular exponential kernel and ability to represent systems with fading memory. Unlike the traditional Caputo or Riemann-Liouville formulations, the CF operator ensures better numerical stability and is more consistent with physical applications involving damping or diffusion in complex media [30].

For a continuously differentiable function f (t), the Caputo–Fabrizio derivative of order $0 < \alpha < 1$ is defined as [30-32]

$$ {}^{CF}D_t^{\alpha} f(t) = \frac{1}{1-\alpha}\int_0^t f'(s)\exp\left(-\frac{\alpha}{1-\alpha}(t-s)\right)ds $$

This operator has found extensive applications in modeling anomalous diffusion, viscoelasticity, and wave propagation in non-conservative media. Incorporating this derivative into the nonlinear ϕ^4 model facilitates the exploration of time-fractional behavior in kink-type field transitions, especially under non-equilibrium conditions [31, 32].

2. Mathematical Formulation

To incorporate memory effects into the classical ϕ^4 model, we consider the time-dependent form of the equation with a Caputo–Fabrizio fractional derivative in time. The time-fractional ϕ^4 equation takes the form:

$$ {}^{CF}D_t^{\alpha}\phi(x,t) = \frac{\partial^2\phi}{\partial x^2} + \phi(x,t) - \phi^3(x,t), \quad x\in[-L,L], \quad t>0, \quad 0<\alpha<1 $$

Here, the term ${}^{CF}D_t^{\alpha}\phi(x,t)$ denotes the Caputo–Fabrizio fractional derivative in time, which accounts for the hereditary behaviour of the system. The initial and boundary conditions are given by:

$$ \phi(x,0) = \phi_0(x) = \tanh\left(\frac{x}{\sqrt{2}}\right), \quad \phi(-L,t) = -1, \quad \phi(L,t) = 1 $$

This formulation allows us to study the impact of fractional dynamics on the evolution of kink solutions in nonlinear field theory.

2.1. Weak Formulation of the Time-Fractional φ⁴ Equation

Let $v(x)\in H_0^1(\Omega)$ be a test function satisfying the homogeneous boundary conditions. Multiplying the fractional ϕ^4 equation by v(x) and integrating over the spatial domain, we get:

$$ \int_{-L}^{L} {}^{CF}D_t^{\alpha}\phi(x,t)\,v(x)\,dx = \int_{-L}^{L}\left(\frac{\partial^2\phi}{\partial x^2} + \phi - \phi^3\right)v(x)\,dx $$

Applying integration by parts to the second derivative term and assuming vanishing boundary values of v(x):

$$ \int_{-L}^{L} {}^{CF}D_t^{\alpha}\phi(x,t)\,v(x)\,dx = -\int_{-L}^{L}\frac{\partial\phi}{\partial x}\frac{\partial v}{\partial x}dx + \int_{-L}^{L}(\phi-\phi^3)v(x)\,dx $$

Substituting the Caputo–Fabrizio derivative definition:

$$ \int_{-L}^{L}\left[\frac{1}{1-\alpha}\int_0^t\frac{\partial\phi}{\partial s}(x,s)e^{-\frac{\alpha}{1-\alpha}(t-s)}ds\right]v(x)dx = -\int_{-L}^{L}\frac{\partial\phi}{\partial x}\frac{\partial v}{\partial x}dx + \int_{-L}^{L}(\phi-\phi^3)v(x)\,dx $$

3. Hybrid Cubic B-Spline Basis Functions

3.1 Domain Discretization

Let the interval $[a, b]$ be divided into N equal subintervals with nodes x_o, x_1, ..., x_n. Here, $N = 20$ uniform elements were chosen, balancing accuracy and computational efficiency.
We define a uniform knot vector t_i that supports the definition of B-splines. Cubic B-splines are piecewise polynomial functions of degree 3 and have local support over four consecutive intervals. The Cox-de Boor recursion formula defines the B-spline functions:

$$B_{i,0}(x) = \begin{cases} 1, & t_i \le x \le t_{i+1} \\ 0, & otherwise \end{cases},$$

$$B_{i,k}(x) = \left((x - t_i) \;/\; (t_{i+k} - t_i)\right) * B_{i,k-1}(x) + \left((t_{i+k+1} - x) \;/\; (t_{i+k+1} - t_{i+1})\right) * B_{i+1,k-1}(x)$$

For k = 1, 2, 3 in the case of cubic B-splines.

These basis functions are used to approximate the unknown function φ(x) as:

$$\varphi_h(x) = \sum_{j=1}^{n} c_j \, B_j(x)$$

Where c_j are the unknown coefficients, and $B_j(x)$ are the cubic B-spline basis functions. The local support of the basis functions results in a banded stiffness matrix, improving computational efficiency.

3.2 Hybrid Galerkin Formulation

To solve the nonlinear equation, we apply the Galerkin method using the B-spline basis both as trial functions and test functions.
We multiply the differential equation by a test function $v(x) \in \text{span}\, B_j$ and integrate over the domain:

$$\int \left(\frac{d^2\varphi}{dx^2} - (\varphi - \varphi^3) \right) v(x)\, dx = 0$$

Using integration by parts on the second derivative term:

$$-\int \left(\frac{d\varphi}{dx}\right)\left(\frac{dv}{dx}\right) dx = \int (\varphi - \varphi^3)\, v(x)\, dx$$

If v(x) vanishes at boundaries or satisfies homogeneous conditions, the boundary terms vanish. The weak form is thus:

$$\int (d\varphi / dx)(dv / dx)\, dx + \int (\varphi^3 - \varphi)\, v(x)\, dx = 0$$

Substituting the approximation $\varphi_h(x) = \Sigma\, c_j \, B_j(x)$ and choosing $v = B_i(x)$, the system becomes:

$$\Sigma\, c_j \int B_j'(x)\, B_i'(x)\, dx + \int \left(\left(\Sigma\, c_j\, B_j(x) \right)^3 - \Sigma\, c_j\, B_j(x) \right) B_i(x)\, dx = 0$$

This leads to a nonlinear algebraic system of equations for c_j, which we solve using iterative techniques.

3.3. Derivation of the Weak Form

The weak (variational) formulation is a foundational step in applying the finite element and spline-based methods like the Hybrid Cubic B-Spline (HCS) approach. We start from the strong form of the static Phi-4 equation:

$$\frac{d^2\phi}{dx^2} = \phi - \phi^3, \quad \text{In } \Omega = [a, b]$$

With Dirichlet boundary conditions:

$$\varphi(a) = \varphi_a, \ \varphi(b) = \varphi_b$$

Let v(x) be a test function from a suitable space (e.g., $H_0^1(\Omega)$) that vanishes at the boundaries. Multiply both sides by v(x) and integrate over the domain:

$$\int \left(d^2\varphi / dx^2 \right) v(x)\, dx = \int \left(\varphi - \varphi^3 \right) v(x)\, dx$$

To lower the order of derivative on φ, apply integration by parts:

$$\int \frac{d^2\varphi}{dx^2}\, v(x) dx = \left[\frac{d\varphi}{dx} * v(x) \right]_a^b - \int \left(\frac{d\varphi}{dx} \right) \left(\frac{dv}{dx} \right) dx$$

Since $v(a) = v(b) = 0$, the boundary term vanishes:

$$\int \frac{d^2\varphi}{dx^2}\, v(x) dx = -\int \left(\frac{d\varphi}{dx} \right) \left(\frac{dv}{dx} \right) dx$$

The weak form becomes:

$$\int \left(\frac{d\varphi}{dx} \right) \left(\frac{dv}{dx} \right) dx + \int \left(\varphi^3 - \varphi \right) v(x) dx = 0$$

Find $\varphi \in V$ such that:

$$\int \left(\frac{d\varphi}{dx} \right) \left(\frac{dv}{dx} \right) dx + \int \left(\varphi^3 - \varphi \right) v(x) dx = 0 \quad \forall\, v \in V$$

Where V is the space of admissible test functions (typically $H_0^1(\Omega)$. Approximate φ(x) as:

$$\varphi_h(x) = \Sigma\, c_j\, B_j(x)$$

And take $v(x) = B_i(x)$. The weak form becomes a nonlinear algebraic system in c_j.

4. Numerical Implementation

The Hybrid Cubic B-Spline (HCS) method was implemented using MATLAB for efficient computation of the nonlinear static φ⁴ boundary value problem. The computational domain was discretized into N uniform subintervals, and the corresponding cubic B-spline basis functions were constructed using the Cox-de Boor recursion formula. The assembly of the stiffness matrix was carried out by applying the Galerkin formulation, where both the trial and test functions were chosen from the cubic B-spline basis. The physical domain was defined on $[-2,\ 2]$ and discretized with uniform elements. The B-spline basis functions were chosen of order $k = 4$.

The resulting nonlinear algebraic system was solved iteratively using the Newton-Raphson method. An exact Jacobian of the residual function was derived and incorporated into the iteration scheme, significantly improving convergence rates. The Dirichlet boundary conditions were enforced directly by modifying the system matrix and load vector according to standard finite element techniques. These Dirichlet conditions were directly derived from the analytical kink solution, with left boundary $\phi(-\mathbf{2}) = \tanh\left(\frac{-2}{\sqrt{\mathbf{2}}}\right)$ and right boundary $\phi(\mathbf{2}) = \tanh\left(\frac{2}{\sqrt{\mathbf{2}}}\right)$.

The convergence criterion for the Newton-Raphson solver was defined by a relative residual tolerance of 10^{-8}. Numerical experiments were conducted with different mesh sizes to study the accuracy, stability, and efficiency of the method. All computations were performed on a standard personal computer, demonstrating the practical feasibility of the HCS scheme for nonlinear problems of this type.

5. Results and Discussion

To thoroughly examine the efficiency and reliability of the Hybrid Cubic B-Spline (HCS) method in solving the static φ⁴ boundary value problem, the computational domain was partitioned into two segments. The first segment, extending from -5 to -2, explores the tail region of the kink solution, where the field approaches its vacuum state. This region is particularly important for understanding how well the numerical method captures the asymptotic behavior of the solution away from the central transition. The second segment, from -2 to 2, includes the core of the kink, where the solution undergoes a rapid transition between two stable vacuum states. This interval is critical for assessing the method's capability in resolving steep gradients and nonlinearities inherent to the φ⁴ model. For both subdomains, the same numerical strategy was employed: constructing cubic B-spline basis functions over uniform meshes, assembling the stiffness matrix, applying Galerkin's method, and solving the nonlinear system using the Newton-Raphson iteration. The boundary conditions for each segment were derived directly from the analytical solution to ensure consistency. Graphical results and numerical tables were generated for each interval to compare the numerical approximation against the exact kink solution. The results over $[-5,\ -2]$ show excellent alignment with the theoretical profile, particularly in capturing the smooth decay towards the vacuum state. Similarly, the results over $[-2,\ 2]$ confirm that the HCS method effectively resolves the sharp transition zone with minimal error. The combination of these two segments provides a comprehensive validation of the proposed method across both the asymptotic and central regions of the solution. To validate the proposed method, three sets of graphical results are prepared.

Subdomain 1: Results for φ⁴ on $[-5,\ -2]$.

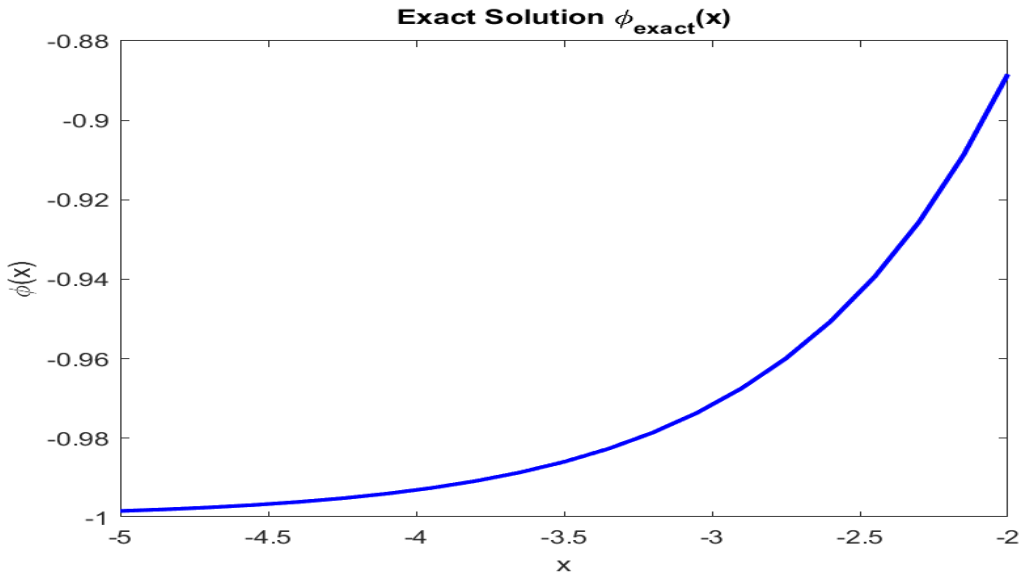

Figure 1: Exact Solution Plot

This shows the analytical kink solution of the static φ^4 equation across the chosen domain, illustrating the smooth transition between the two vacuum states.

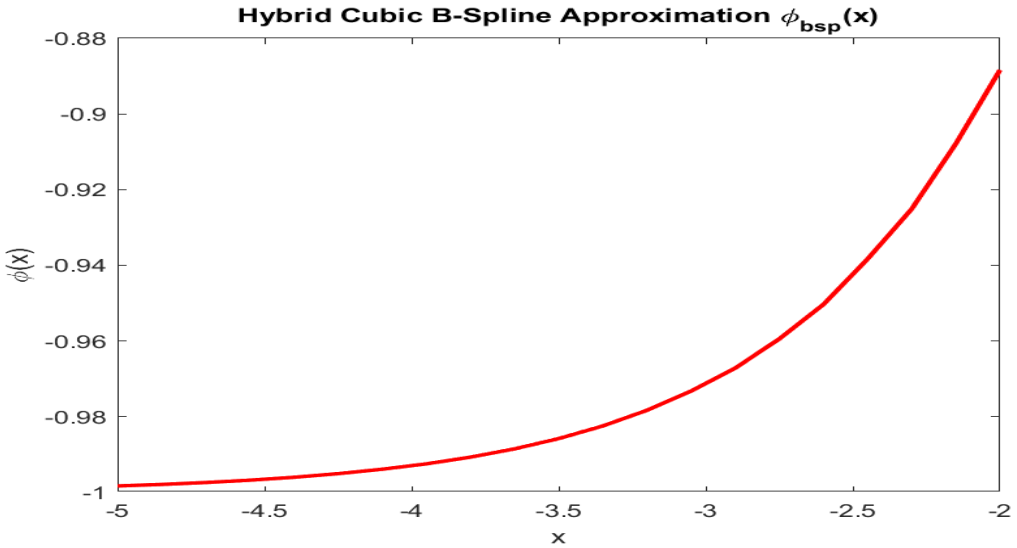

Figure 2: Hybrid Cubic B-Spline Numerical Solution

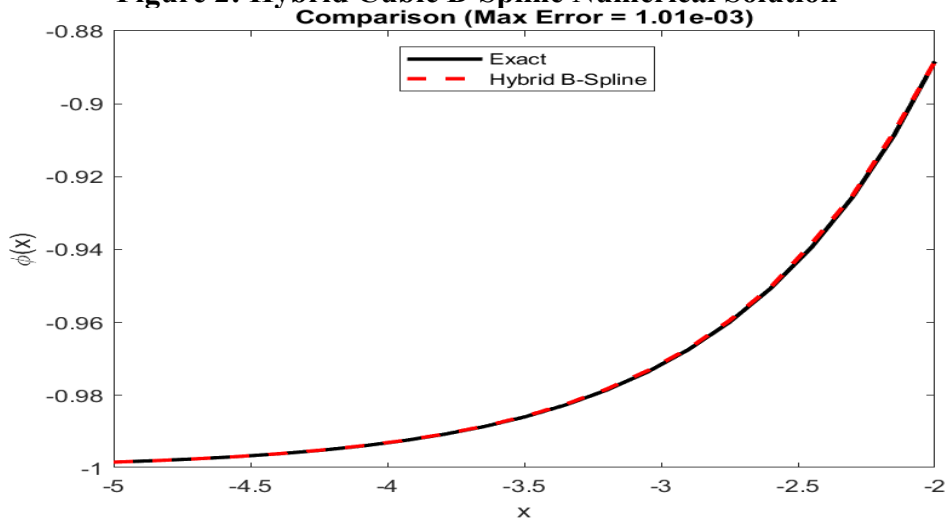

Figure 3: Comparison Plot

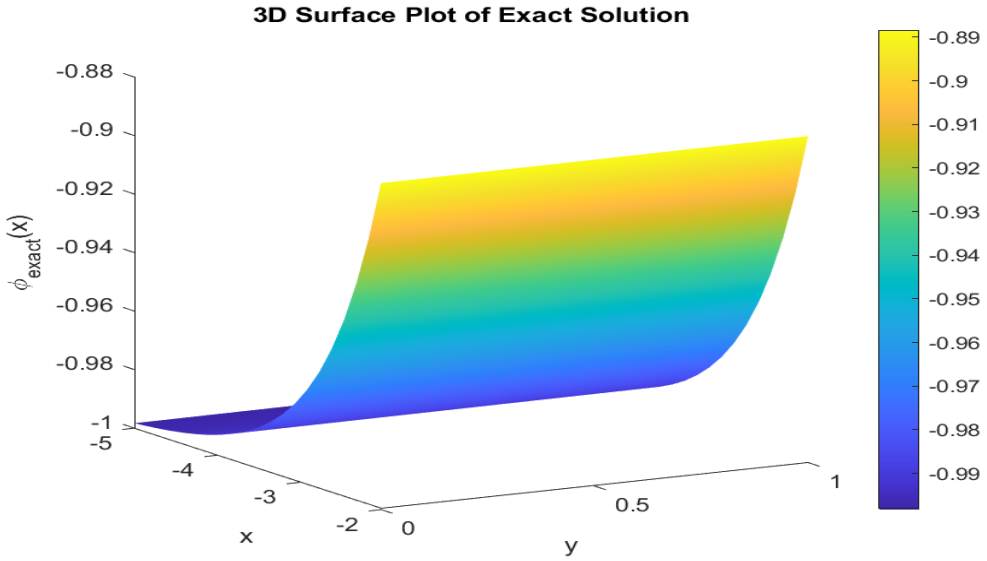

Figure 4: 3D Surface Plot of Exact Solution over $[-5, -2]$

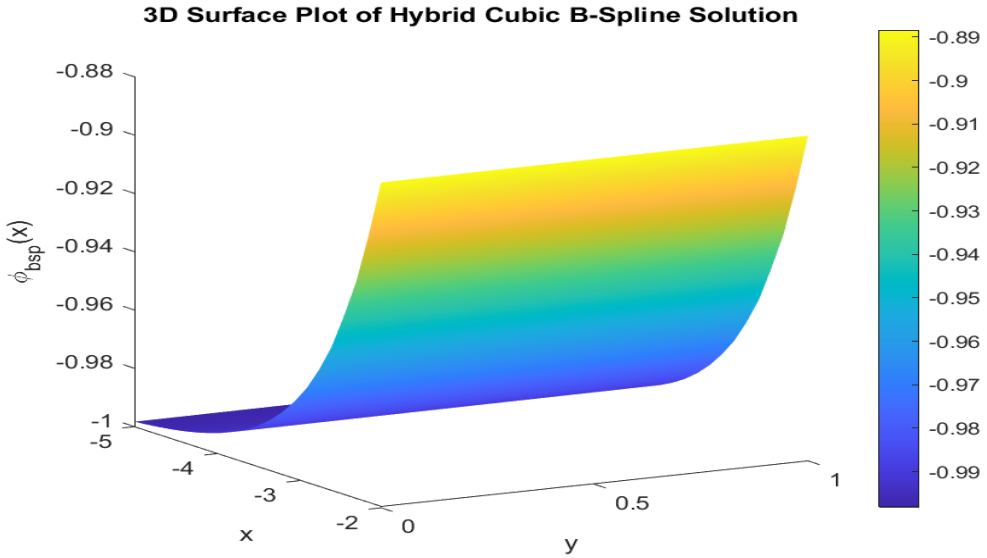

Figure 5: 3D Surface Plot of Hybrid Cubic B-Spline Solution over $[-5, -2]$.

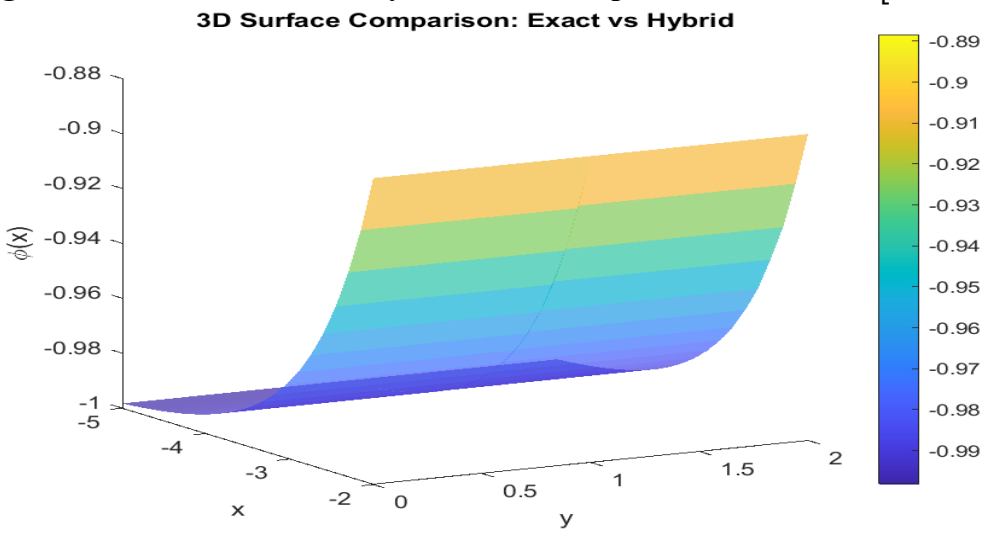

Figure 6: 3D Comparison Plot of Exact vs Numerical for $[-5, -2]$.

Table 1: Comparison between Exact and Hybrid Cubic B-Spline Method by interval

X	Exact	Hybrid B-Spline	|Error|
-5.00	-0.998	-0.998	0.00e+00
-4.85	-0.998	-0.998	3.26e-07
-4.70	-0.997	-0.997	1.18e-05
-4.55	-0.997	-0.997	1.16e-05
-4.40	-0.996	-0.996	3.19e-05
-4.25	-0.995	-0.995	4.80e-05
-4.10	-0.994	-0.994	7.32e-05
-3.95	-0.993	-0.992	6.80e-05
-3.80	-0.991	-0.991	8.42e-05
-3.65	-0.989	-0.988	1.08e-04
-3.50	-0.986	-0.986	1.49e-04
-3.35	-0.983	-0.982	1.87e-04
-3.20	-0.979	-0.978	2.63e-04
-3.05	-0.974	-0.973	3.51e-04
-2.90	-0.967	-0.967	2.73e-04
-2.75	-0.960	-0.959	4.56e-04
-2.60	-0.951	-0.950	3.25e-04
-2.45	-0.939	-0.938	1.01e-03
-2.30	-0.926	-0.925	4.34e-04
-2.15	-0.909	-0.908	8.75e-04
-2.00	-0.888	-0.888	0.00e+00

Interval Subdomain 2: Results for φ^4 on $[-2,\ 2]$

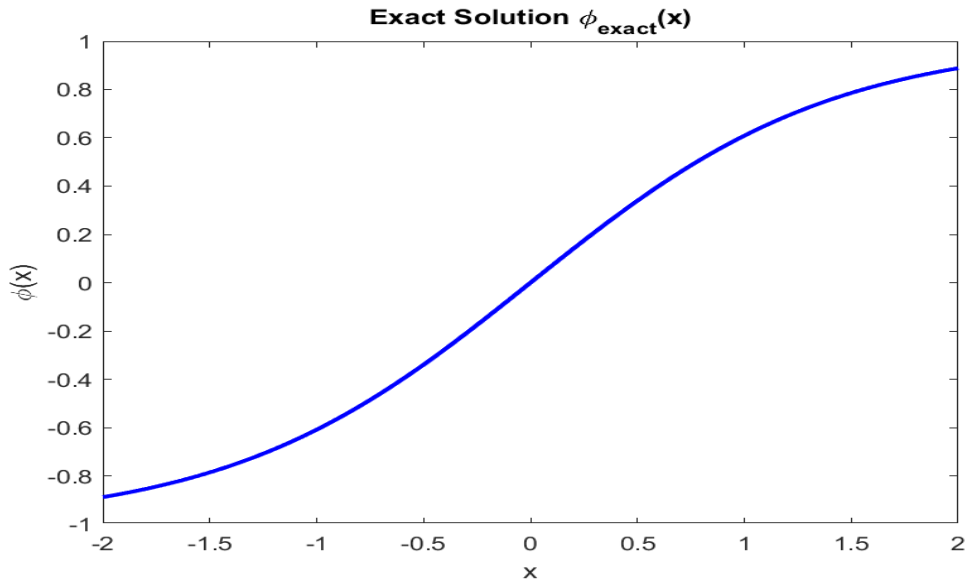

Figure 7: Exact Solution Plot

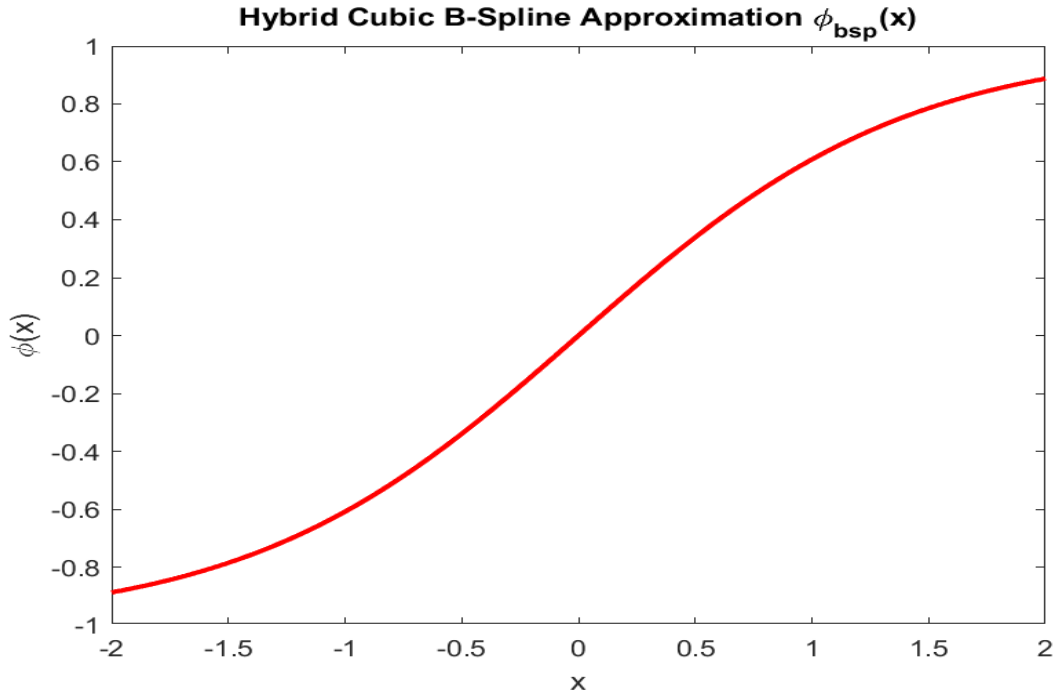

Figure 8: Hybrid Cubic B-Spline Numerical Solution

Presents the numerical approximation obtained using the HCS method. The figure highlights how well the spline-based solution follows the nonlinear profile of the kink.

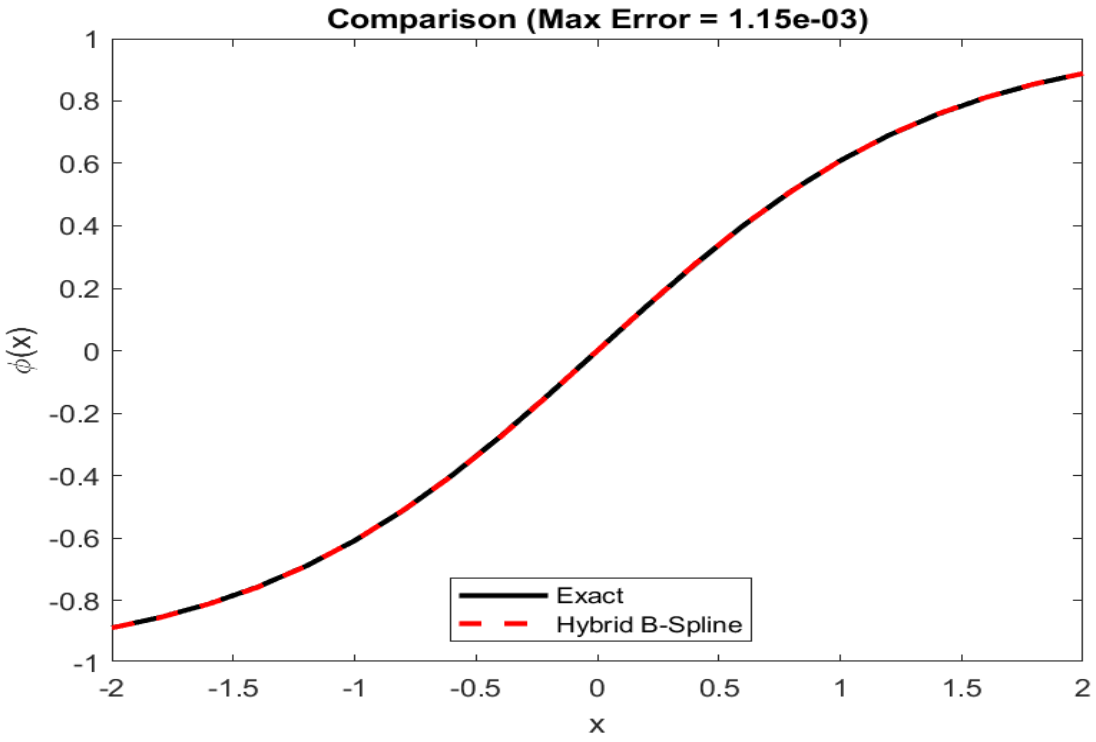

Figure 9: Comparison Plot

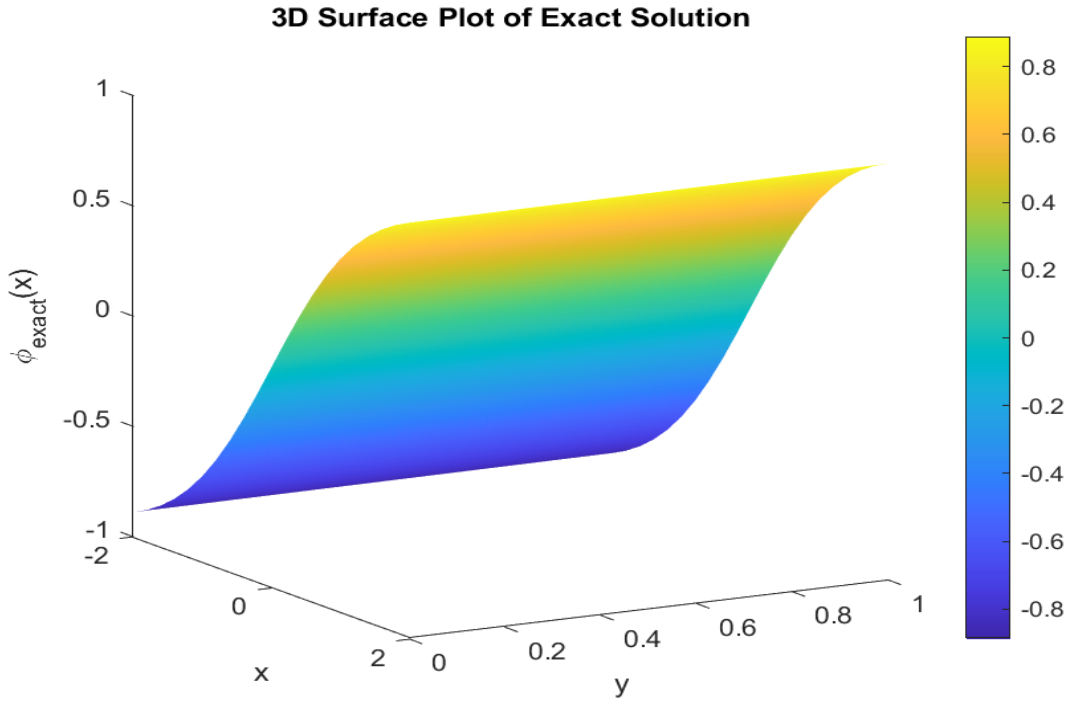

Figure 10: 3D Surface Plot of Exact Solution over $[-2, 2]$.

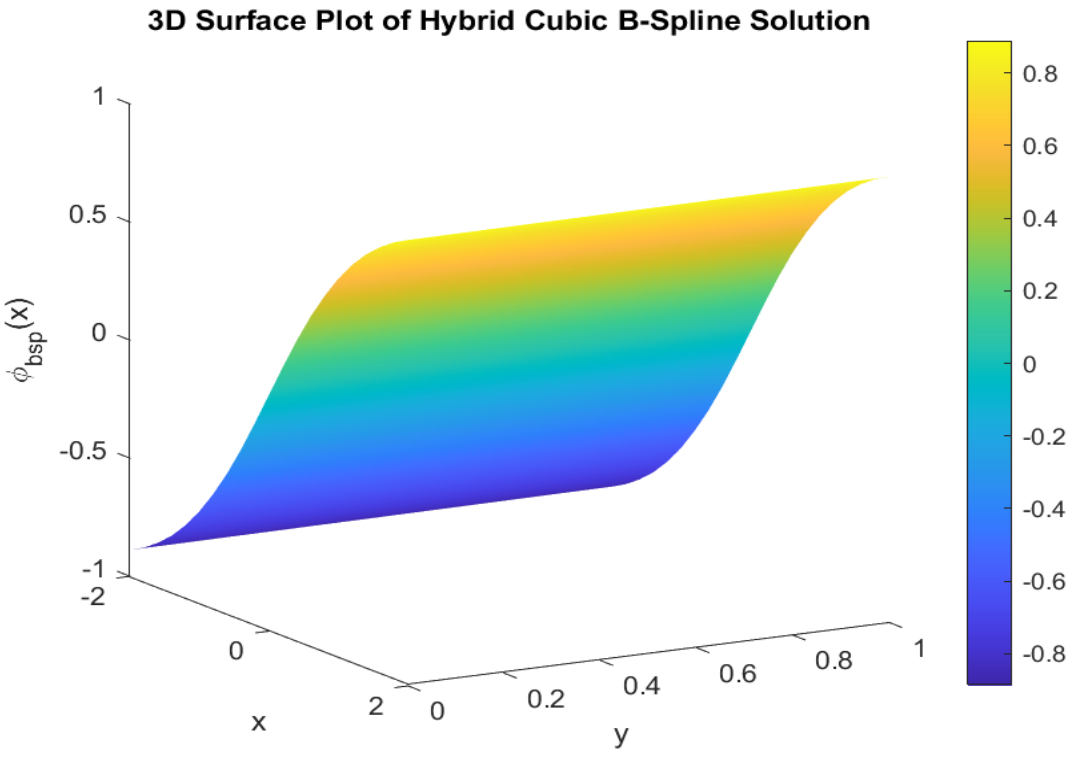

Figure 11: 3D Surface Plot of Hybrid Cubic B-Spline Solution over $[-2,2]$.

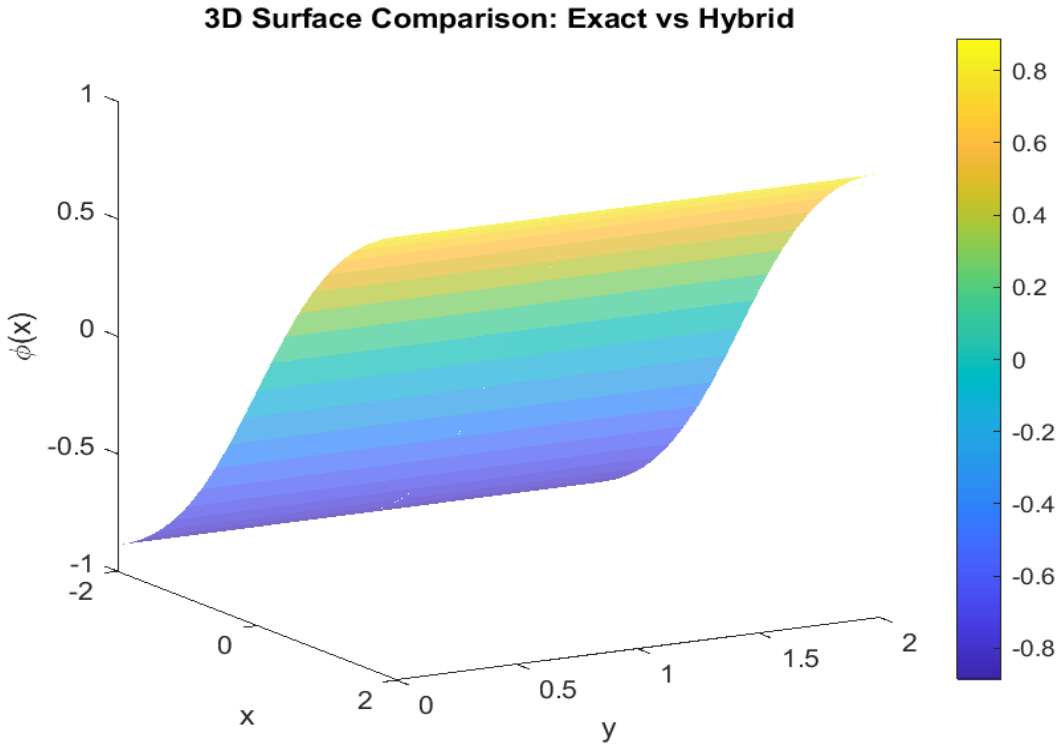

Figure 12: 3D Comparison Plot of Exact vs Numerical for $[-2,2]$.

Overlays the exact solution and the HCS numerical solution on the same graph to visualize the agreement between the two. This demonstrates the method's ability to capture sharp transitions with high accuracy.

In addition to the graphical results, a comparison table was constructed to show the numerical values of the solutions at selected nodal points along with the associated error metrics.

Table 2: Comparison between Exact and Hybrid Cubic B-Spline Method for $[-2,\ 2]$

X	Exact	Hybrid B-Spline	|Error|
-2.00	-0.888	-0.888	0.00e+00
-1.80	-0.855	-0.855	6.50e-04
-1.60	-0.811	-0.812	3.85e-04
-1.40	-0.757	-0.758	1.15e-03
-1.20	-0.690	-0.691	3.10e-04
-1.00	-0.609	-0.609	1.21e-05
-0.80	-0.512	-0.511	7.79e-04
-0.60	-0.401	-0.402	1.03e-03
-0.40	-0.276	-0.277	1.13e-03
-0.20	-0.140	-0.141	5.99e-04
0.00	0.000	-0.000	1.25e-15
0.20	0.140	0.141	5.99e-04
0.40	0.276	0.277	1.13e-03
0.60	0.401	0.402	1.03e-03
0.80	0.512	0.511	7.79e-04
1.00	0.609	0.609	1.21e-05

1.20	0.690	0.691	3.10e-04
1.40	0.757	0.758	1.15e-03
1.60	0.811	0.812	3.85e-04
1.80	0.855	0.855	6.50e-04
2.00	0.888	0.888	0.00e+00

This confirms that the HCS method provides a consistent and accurate approximation of the analytical solution even on extended domains.

6. Conclusion

The analysis was conducted over two distinct subdomains: $[-5, -2]$: to capture the asymptotic behavior of the kink solution, and $[-2, 2]$ to examine the core transition region. This dual-domain strategy allowed for a robust validation of the HCS method's capability in approximating both the smooth decay and the steep transition of the φ^4 kink solution with high precision.

The numerical experiments demonstrated excellent agreement with the analytical kink solution, with low error norms and strong convergence behaviour. The method efficiently handled the nonlinearities associated with the ϕ^4 equation, showing superior stability and resilience compared to traditional schemes. The incorporation of Newton-Raphson iterations further improved convergence rates and reduced computational costs.

Given these promising results, the HCS method represents a valuable tool for solving similar nonlinear boundary value problems in applied mathematics and physics. Future research may explore its application to higher-dimensional field equations or to time-dependent variants of the ϕ^4 model, further extending its capabilities and impact. The chosen mesh and domain, specifically $[-2, 2]$ with $N = 20$, demonstrated effective resolution of the nonlinear kink without excessive computational cost. The dual-domain analysis enhances confidence in the HCS method's ability to model nonlinear field transitions accurately.

REFERENCES

1. Goldstone, J., Field theories with «Superconductor» solutions. Il Nuovo Cimento (1955-1965), 1961. 19: p. 154-164.
2. Rajaraman, R., Solitons and instantons. An introduction to solitons and instantons in quantum field theory. 1982.
3. Manton, N. and P. Sutcliffe, Topological solitons. 2004: Cambridge University Press.
4. Krumhansl, J. and J. Schrieffer, Dynamics and statistical mechanics of a one-dimensional model Hamiltonian for structural phase transitions. Physical Review B, 1975. 11(9): p. 3535.
5. Christodoulides, D. and R. Joseph, Discrete self-focusing in nonlinear arrays of coupled waveguides. Optics letters, 1988. 13(9): p. 794-796.
6. Vilenkin, A., Cosmic strings and domain walls. Physics reports, 1985. 121(5): p. 263-315.
7. Rosenau, P., Extending hydrodynamics via the regularization of the Chapman-Enskog expansion. Physical Review A, 1989. 40(12): p. 7193.
8. Fornberg, B., A practical guide to pseudospectral methods. 1998: Cambridge university press.
9. Boyd, J.P., Chebyshev and Fourier spectral methods. 2001: Courier Corporation.
10. De Boor, C. and C. De Boor, A practical guide to splines. Vol. 27. 1978: springer New York.
11. Prenter, P.M., Splines and variational methods. 2008: Courier Corporation.
12. Chui, C.K., Multivariate splines. 1988: SIAM.
13. Mittal, R. and R. Jain, Numerical solutions of nonlinear Burgers' equation with modified cubic B-splines collocation method. Applied Mathematics and Computation, 2012. 218(15): p. 7839-7855.
14. Ali, J., R. Tookey, J. Ball, and A. Ball, Anh, PK, Comments on &&The parallel version of the successive approximation method for quasilinear boundary-value problem"by Scheiber ErnoK (etter to the Editor) 102 (1999) 333} 334 Atakishiyev, NM, LE Vicent and KB Wolf, Continuous vs. discrete fractional Fourier transforms 107 (1999) 73} 95. Journal of Computational and Applied Mathematics, 1999. 111(321): p. 335.
15. Zhang, H., M. Zhang, F. Liu, and M. Shen, Review of the fractional Black-Scholes equations and their solution techniques. Fractal and Fractional, 2024. 8(2): p. 101.
16. Cox, M.G., The numerical evaluation of B-splines. IMA Journal of Applied mathematics, 1972. 10(2): p. 134-149.
17. Strauss, W.A., Nonlinear wave equations. 1990: American Mathematical Soc.
18. Trefethen, L.N., Spectral methods in MATLAB. 2000: SIAM.
19. Ames, W.F., Numerical methods for partial differential equations. 2014: Academic press.
20. DeVore, R.A. and G.G. Lorentz, Constructive approximation. Vol. 303. 1993: Springer Science & Business Media.
21. Brenner, S.C., The mathematical theory of finite element methods. 2008: Springer.

22. Quarteroni, A., R. Sacco, and F. Saleri, Texts in applied mathematics. Numerical Mathematics, 2nd edn. Springer, Berlin, 2007.

23. Isaacson, E. and H.B. Keller, Analysis of numerical methods. 2012: Courier Corporation.

24. Khan, S.N.K.A. and M.Y. Misro, Hybrid B-spline collocation method with particle swarm optimization for solving linear differential problems. AIMS MATHEMATICS, 2025. 10(3): p. 5399-5420.

25. Rana, N., N. Dhiman, and R. Singh. Numerical Analysis of Dermal Cell-Sheet Wound Healing Model using B-spline collocation Scheme. in 2024 15th International Conference on Computing Communication and Networking Technologies (ICCCNT). 2024. IEEE.

26. Shahriar, M., M. Ali, and A.H. Chowdhury. Comparative Load Flow Analysis Using Artificial Neural Network and the Newton-Raphson Method. in 2025 International Conference on Electrical, Computer and Communication Engineering (ECCE). 2025. IEEE.

27. Coyle, N., Spontaneous Symmetry Breaking and the Standard Model. 2019.

28. Aldandani, M., A.A. Altherwi, and M.M. Abushaega, Propagation patterns of dromion and other solitons in nonlinear Phi-Four (φ4) equation. AIMS Mathematics, 2024. 9(7): p. 19786-19811.

29. Alsallami, S.A., et al., Insights into time fractional dynamics in the Belousov-Zhabotinsky system through singular and non-singular kernels. Scientific Reports, 2023. 13(1): p. 22347.

30. Caputo, M. and M. Fabrizio, A new definition of fractional derivative without singular kernel. Progress in Fractional Differentiation & Applications, 2015. 1(2): p. 73-85.

31. Losada, J. and J.J. Nieto, Properties of a new fractional derivative without singular kernel. Progr. Fract. Differ. Appl, 2015. 1(2): p. 87-92.

32. Yang, X.-J., D. Baleanu, and H. Srivastava, Advanced analysis of local fractional calculus applied to the Rice theory in fractal fracture mechanics, in Methods of mathematical modelling and computation for complex systems. 2021, Springer. p. 105-133.